

1

Asphericity Effects in Supernovae

P. Höflich, C. Gerardy, R. Quimby
University of Texas, Austin, TX 78712, USA

Abstract. We present a brief summary of asphericity effects in thermonuclear and core collapse supernovae (SN), and how to distinguish the underlying physics by their observable signatures. Electron scattering is the dominant process to produce polarization which is one of the main diagnostical tools. Asphericities result in a directional dependence of the luminosity which has direct implications for the use of SNe in cosmology. For core collapse SNe, the current observations and their interpretations suggest that the explosion mechanism itself is highly aspherical with a well defined axis and, typically, axis ratios of 2 to 3. Asymmetric density/chemical distributions and off-center energy depositions have been identified as crucial for the interpretation of the polarization P . For thermonuclear SNe, polarization turned out to be an order of magnitude smaller strongly supporting rather spherical, radially stratified envelopes. Nevertheless, asymmetries have been recognized as important signatures to probe A) for the signatures of the progenitor system, B) the global asymmetry with well defined axis, likely to be caused by rotation of an accreting white dwarf or merging WDs, and C) possible remains of the deflagration pattern.

1.1 Introduction

During the last decade, advances in observational, theoretical and computational astronomy have provided new insights into the nature and physics of SNe and gamma-ray bursts. Due to the extreme brightness of these events, they are expected to continue to play important role in cosmology. SNe Ia allowed good measurements of the Hubble constant both by statistical methods and theoretical models. SNe Ia have provided one of the strong evidences for a non-zero cosmological constant, and will be used to probe the nature of the dark energy. In the future, core collapse SNe and the related GRBs may become the tool of choice to probe the very first generation of stars. The multidimensional nature of these objects has been realized and it has become obvious that measurements of asymmetries and their understanding is a key for understanding of both SNe and GRBs. In this contribution, we want to give a brief overview on the observable consequences of asphericity including a directional dependence of the luminosity with a special emphasis on polarization in Thomson scattering dominated envelopes. In a first part, we want to give a brief introduction to the configurations which produce polarization. Subsequently, we present examples for various mechanisms which produce polarization in core collapse and thermonu-

2 Asphericity Effects in Supernovae

clear SNe. It is beyond the scope to present a review of the current literature. A more general overview about the physics core collapse SNe with references to the general literature can be found in Höflich et al. (2002). For thermonuclear SNe on scenarios and details of the nuclear burning front, we want to refer Höflich et al. (2003), and Hillebrandt & Niemeyer (2000), Khokhlov (2001) and Gamezo & Khokhlov (this volume), respectively. W will focus on the theoretical aspects. For a complementary discussion of the observations, see Wang(this volume).

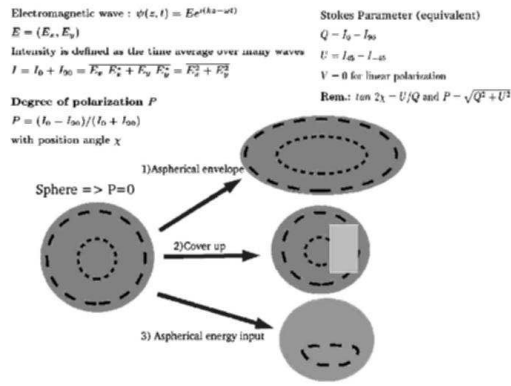


Fig. 1.1. Definition of the polarization and schematic diagram for its production. The dotted lines give the main orientation of the electrical vectors. For an unresolved sphere, the components cancel out (from Höflich 1995).

1.2 General

Asymmetry can be probed by direct imaging of ejecta of the remnants, e.g. in SN1987A (Wang et al. 2002, Höflich et al. 2001b), or Cas A (Fesen & Gunderson 1997), proper motions of neutron stars (Strom et al. 1995), or, more general, by polarization measurements during the early phase of the expansion. In SN, polarization is mainly produced by Thomson scattering of photons in an aspherical configuration. It can be caused by asymmetries in the density, abundances or excitation structure of an envelope. In general, the ejecta cannot be spatially resolved. Although the light from different parts of a spherical disk is polarized, the resulting polarization \bar{P} is zero for the integrated light (Fig. 1.1). To produce \bar{P} , three basic configurations may be considered, in which I) the photosphere is aspherical, II) parts of the disk are shaded, and III) the envelope may be illuminated by an off-center light source. In case II, the shading may be either by a broad-band absorber such as dust or a specific line opacity. In the latter case, this would produce a change of \bar{P} in a narrow line range (Figs. 1.2). In reality, a combination of all cases may be realized. Note that quantitative analyzes of SNe need to take into account that the continua and lines are not formed in the same layers. Polarization carries the information about the apparent, global asymmetries. E.g., it increases with increasing axis ratios in ellipsoidal geometries or off-center energy sources but decreases due to multiple scattering (the optical depth) or steep density profiles. Observed size of P depends also on the position of the observer relative to the object. For a detailed discussion see Höflich (1991, 1995). As a consequence, the interpretation of polarization data are not unique. Another problem is due to polarization by the interstellar medium. In

parts, these limitations can be overcome by spectropolarimetry and time series of observations which provides additional information due to spectral features (see Fig. 1.2) and their evolution. Still, the use of consistent physical models is mandatory to further constrain the variety of interpretation.

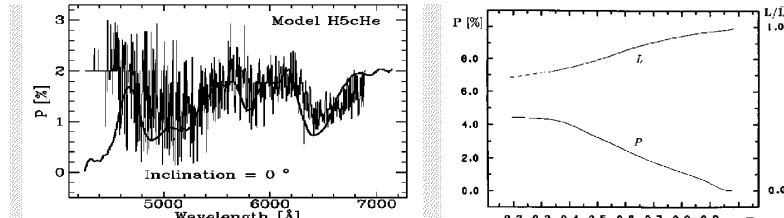


Fig. 1.2. Polarization spectrum for SN1993J for an axis ratio of 1/2 for an oblate ellipsoid in comparison with observations by Trammell et al. (1993) (left plot). On the right, the dependence of the continuum polarization (right) and directional dependence of the luminosity is shown as a function axis ratios for oblate ellipsoids seen from the equator (from Höflich, 1991 & Höflich et al. 1995).

1.3 Core Collapse Supernovae

In recent years, there has been a mounting evidence that the explosions of massive stars (core collapse SNe) are highly aspherical. The spectra (e.g., SN87A, SN93J, SN94I, SN99em, SN02ap) are significantly polarized at a level of 0.5 to 3 % (Méndez et al. 1988, Cropper et al. 1988, Höflich 1991, Jeffrey 1991) indicating aspherical envelopes by factors of up to 2 (see Fig. 1.2). The degree of polarization tends to vary inversely with the mass of the hydrogen envelope, being maximum for Type Ib/c events with no hydrogen (Wang et al. 2001). For SNeII, Leonard et al. (2000) and Wang et al. (2001) showed that the polarization and, thus, the asphericity increase with time. The orientation of the polarization vector tends to stay constant both in time and with wavelength. This implies that there is a global symmetry axis in the ejecta. Both trends suggest a connection of the asymmetries with the central engine which may be understood in terms of jet-induced explosions (Khokhlov et al. 1999, Höflich et al. 1998, 2002), or pulsational modes in neutrino driven explosions (Scheck et al. 2003).

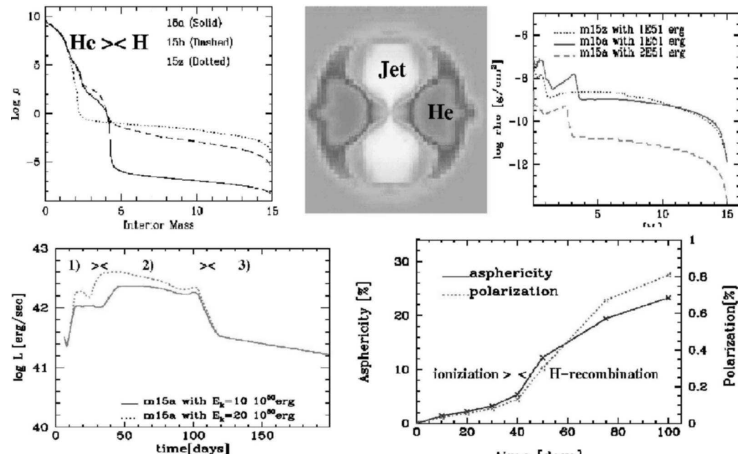


Fig. 1.3. Polarization produced by an aspherical, chemical distribution for an extreme SN IIp model such as SN1999em (see text).

4 Asphericity Effects in Supernovae

However, even strongly asymmetric explosions do not produce asymmetries in the massive hydrogen-rich envelopes of SNeII which are sufficiently large to explain the polarization observed in SN1987A or SN1999em. Aspherical excitation by hard radiation is found to be crucial. As example, the extreme SNIp 1999em is shown in Fig. 1.3 and, for details, see Höflich et al. (2002). Our calculations of the initial stage of the explosion employ 3D hydrodynamics. The explosion of a star with 15 solar masses is triggered by a low velocity, high density jet/bipolar outflow which delivers a explosion energies of of 1 and $2 \times 10^{51} \text{ erg}$. The jet from the central engine stalls after about 250 seconds, and the abundance distribution freezes out in the expanding envelope. The resulting distribution of the the He-rich layers is given in Fig. 1.3. The colors white, yellow, green, blue and red correspond to He mass fractions of 0., 0.18, 0.36, 0.72, and 1., respectively. The composition of the jet-region consists of a mixture of heavy elements with about $0.07 M_{\odot}$ of radioactive ^{56}Ni . After about 100 seconds, the expansion of the envelope becomes spherical. Thus, for times larger than 250 seconds, the explosion has been followed in 1-D up to the phase of homologous expansion. In the upper, right panel, the density distribution is given at about 5 days after the explosion. The steep gradients in the density in the upper right and left panels are located at the interface between the He-core and the H-rich mantel. In the lower, left panel, the resulting bolometric LCs are given for explosion energies of $2\text{E}51\text{erg}$ (dotted line) and $1\text{E}51\text{erg}$, respectively. Based on full 3-D calculations for the radiation & γ -ray transport, we have calculated the location of the recombination front (in NLTE) as a function of time. The resulting shape of the photosphere is always prolate. The corresponding axis ratio and the polarization seen from the equator are shown (lower, right panel). Note the strong increase of the asphericity after the onset of the recombination phase between day 30 to 40 (Höflich et al. 2002). For the polarization in a massive, H-rich envelope, P seems to be directly linked to the recombination process and asymmetric excitation.

1.4 Thermonuclear Explosions

For thermonuclear explosions, polarization turned out to be an important tool to probe for A) the global asymmetry caused by the WD, i.e. the continuum component, B) for the signatures of the progenitor system, and C) possible remains of the deflagration pattern produced during the early phase of nuclear burning.

Case A: In general, the maximum, continuum polarization is about an order of magnitude smaller than in core collapse SNe and it is decreasing with time but, again, with a well defined axis of symmetry (e.g. Wang et al. 2003). This decrease occurs despite a significant contribution of electron scattering to the opacity till about 1 to 2 weeks after the explosion. Overall, the objects are rather spherical as could be expected for thermonuclear explosions of a WD. For the subluminous SN1999by, the continuum was polarized up to about 0.7 % (Howell et al. 2001). The well defined axis can be understood in the framework of rotating WDs which may be a consequence the accretion process in a binary system or the merging of two WDs. For the strongly subluminous SN 1999by, the accretion on an accreting WD is clearly favored from the analysis of light curves and spectra (Fig. 1.4). Its unusually high continuum polarization may suggest a correlation between the subluminosity and its low Ni production, i.e. the propagation of the nuclear burning front.

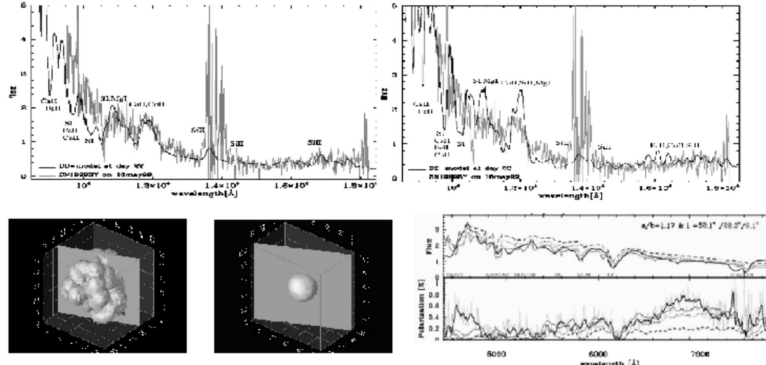


Fig. 1.4. Analysis of the subluminous SN1999by using a combination of flux and polarization data. **Upper panel:** Comparison of the NIR spectrum on May 16 (left) with a spherical, subluminous delayed detonation model. For this object, the spectra are formed in layers of explosive carbon and incomplete silicon burning up to about 2 weeks after maximum light. This is in strict contrast to normal bright SNe Ia where the photosphere enters layers of complete Si burning already at about maximum light. On the right, we show a comparison of the observed and theoretical spectrum if we impose mixing of the inner $0.7 M_{\odot}$ as it can be expected based on detailed 3-D deflagration models (Khokhlov, 2001). Strong homogeneous mixing of the inner layers can be ruled out because the excess excitation of intermediate mass elements and the absorption by iron-group elements (from Höflich et al. 2002). **Lower, left panel:** Energy deposition by γ -rays at day 1 (left) and 23 (right) based on our full 3-D MC gamma ray transport based on a ^{56}Ni distribution of a typical deflagration models. The diameter of the WD is normalized to 100. At about day 23, the energy deposition is not confined to the radioactive ^{56}Ni ruling out clumpiness as a solution to the problem mentioned above (from Höflich 2002). **Lower, right panel:** Optical flux and polarization spectra at day 15 after the explosion for the subluminous 3-D delayed-detonation model in comparison with the SN1999by at about maximum light. The interstellar component of P has been determined to $P = 0.25\%$ with a polarization angle of 140° . The observed flux and the smoothed polarization spectra are the solid black lines. The light grey line is the original data for P at a resolution of 12.5 \AA . In the observations, the polarization angle is constant indicating rotational symmetry of the envelope. The structure of the spherical model has been mapped into oblate ellipsoids with axis ratios A/B of 1.17 (from Howell, Höflich, Wang & Wheeler 2001).

Case B: Interaction with the circumstellar environment may be detected by the appearance of a high velocity component in Ca II (Fig. 1.5). In SN1994D, it may be understood as an ionization effect when Ca III recombines to CaII and, thus, forming two, radially separated features (Höflich et al. 1998, Hatano et al. 2001). Alternatively, double features of CaII may be attributed to abundance pattern (Fisher et al. 1997). The observed polarization in SN2001el was high in Ca II clearly identifying this feature as a morphologically distinct pattern but its origin remained open (Wang et al. 2003, Kasen et al. 2003). Based on a detailed analysis of SN2003du, Gerardy et al. (2003) showed that this feature can be understood in the framework of the interaction between the SN ejecta and its H-rich nearby surroundings.

Case C: Wang et al. (1998) showed that the observed polarization pattern may be consistent with chemical inhomogeneities at the Si/Ni interface as can be expected

6 Asphericity Effects in Supernovae

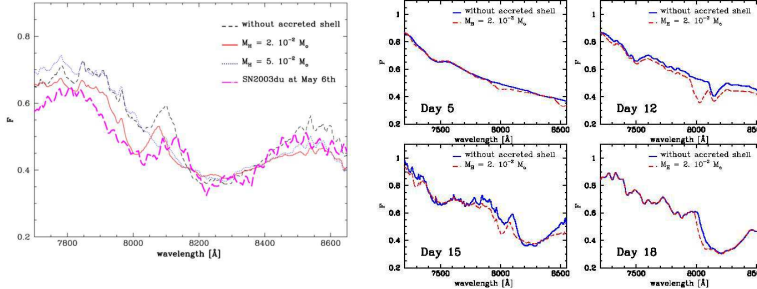


Fig. 1.5. CaII IR feature observed in SN 2003du on May 6 in comparison with theoretical models at about 15 days after the explosion, and its evolution with time. The models are based on a delayed detonation model which interacted with a H-rich shell of 0.02 and 0.05 M_{\odot} during the early phase of the explosion. The dominant signature of this interaction is the appearance of a secondary, high velocity Ca II feature or, for high shell masses, a persistent high velocity component in a broad Ca II line. Without ongoing interaction, no H or He lines are detectable. Note that, even without a shell, a secondary Ca II feature can be seen for a period of 2 to 3 days during the phase when Ca III recombines to Ca II emphasizing the importance of a good time coverage for the observations.

from 3-D deflagration models. However, this detection was on a 1σ level, and needs to be confirmed in other objects.

References

Cropper M., Bailey J., McCowage J., Cannon R., Couch W. 1988, MNRAS 231, 685
 Fesen, R. A. & Gunderson, K. S. 1996, ApJ, 470, 967
 Fisher A., Branch D., Nugent P., Baron E. 1997, 481L, 89
 Gerardy C., Höflich P., Quimby R., Wang L. + the HET-SN team 2003, ApJ, submitted
 Hatano K., Branch D., Lentz E.J., Baron E., Filippenko A. V., Garnavich P. 2000, ApJ 543, L94
 Hillebrandt, W., Niemeyer, J. 2000, ARAA 38, 191
 Höflich, P. 1991 A&A 246, 481
 Höflich, P. 1995, ApJ 443, 89
 Höflich P., Wheeler, J.C., Hines, D., Trammell S. 1995, ApJ 459, 307
 Höflich, P., Khokhlov A., Wang L., 2002, AIP-Publ. 586, p. 459 & astro-ph/0104025
 Höflich, P., Gerardy, C., Linder, E., & Marion, H. 2003, in: Stellar Candles, eds. Gieren et al., Lecture Notes in Physics, Springer Press, in press & astro-ph/0301334
 Howell A., Höflich P., Wang L., Wheeler J. C. 2001, ApJ 556, 302
 Jeffrey D.J., 1991, ApJ, 375, 264
 Kasen, D., Nugent, P., Wang, L., Howell, A., Wheeler, J. C., Höflich, P., Baade, D., Baron, E., Hauschildt, P. 2003, ApJ , in press & astro-ph/0301312
 Khokhlov, A. 2001, astro-ph/0008463
 Leonard D.C., Filippenko, A.V., Barth A.J., Matheson T. 2000, ApJ 536, 239
 Mendez R.H. et al. 1977, ApJ 334, 295
 Scheck L., Plewa T., Janka H.-T., Kifonidis K., Müller E. 2003, Phys.Rev.Let, submitted
 Strom R., Johnston H.M., Verbunt F., Aschenbach B. 1995, Nature, 373, 587
 Trammell S., Hines D., Wheeler J.C. 1993, ApJ 414, 21
 Wang L., Wheeler J.C., Li Z., Clocchiatti A., 1996, ApJ 467, 435
 Wang L., Howell A., Höflich P., Wheeler C. 2001, ApJ 550, 1030
 Wang L., Baade D., Höflich P., Wheeler C., Fransson C., Lundqvist P. 2002, ApJ, submitted
 Wang L., et al. 2002b, ApJ Let., in press & astro-ph/0205337
 Wang, L., Baade, D., Höflich, P., Khokhlov, A., Wheeler, J. C., Kasen, D., Nugent P., Perlmutter S., Fransson C., Lundqvist P. 2003, ApJ 591, 1110

1.4 Thermonuclear Explosions

7

Wang, L., Baade, D., Höflich, P., Wheeler, J. C., Kawabata, K., Nomoto, K. 2003, ApJ, submitted